Synthesis and Characterization of Perfluorinated Acrylate–Methyl Methacrylate Copolymers

Tuba Çakır Çanak, Esin Hamuryudan, İ. Ersin Serhatlı

Department of Chemistry, Istanbul Technical University, Maslak 34469, Istanbul, Turkey
Correspondence to: İ. E. Serhatlı (E-mail: serhatli@itu.edu.tr)

ABSTRACT: A novel perfluorinated acrylic monomer 3,5-bis(perfluorobenzyloxy)benzyl acrylate (FM) with perfluorinated aromatic units was synthesized with 3,5-bis(perfluorobenzyl)oxybenzyl alcohol, acryloyl chloride, and triethylamine. Copolymers of FM monomer with methyl methacrylate (MMA) were prepared via free-radical polymerization at 80°C in toluene with 2,2′-azobisisobutyronitrile as the initiator. The obtained copolymers were characterized by ^{1}H-NMR and gel permeation chromatography. The monomer reactivity ratios for the monomer pair were calculated with the extended Kelen–Tüdos method. The reactivity ratios were found to be $r_1 = 0.38$ for FM, $r_2 = 1.11$ for MMA, and $r_1 r_2 < 1$ for the pair FM–MMA. This shows that the system proceeded as random copolymerization. The thermal behavior of the copolymers was investigated by thermogravimetric analysis and differential scanning calorimetry (DSC). The copolymers had only one glass-transition temperature, which changed from 46 to 78°C depending on the copolymer composition. Melting endotherms were not observed in the DSC traces; this indicated that all of the copolymers were completely amorphous. Copolymer films were prepared by spin coating, and contact angle measurements of water and ethylene glycol on the films indicated a high degree of hydrophobicity. © 2012 Wiley Periodicals, Inc. J. Appl. Polym. Sci. 000: 000–000, 2012

INTRODUCTION

Fluorination, which is the displacement of fluorine atoms with hydrogen, has been explored as a chemical modification for several classes of materials, with numerous attractive features mainly due to the special properties of the small halogen atom; these features include a high electronegativity and the strength of the C—F bond. Because of their small size, fluorine atoms can shield a fluorinated carbon atom without any steric hindrance. This results in a low intermolecular force and, hence, a low surface tension in the fluoropolymers.[1] On the basis of these features, several improvements of the material properties can be expected. Taking advantage of the low surface energy of fluoropolymers makes them useful in a number of applications. Fluoropolymers show resistance to oils, water, and soils and, therefore, are used commonly in coating applications and the textile and carpet industries. Other common uses include non-stick cookware, car finishes, cosmetics, and pharmaceutical applications.[2,3]

In addition, both the overall surface free energy and the coefficient of friction of the system are reduced by the particular introduction of a fluorinated component into a polymer chain.[4,5] These polymers are applied to different surfaces and manufac-

tured into thin films. Such heterophase structures have resulted in a variety of additional materials with technological promise because of their ability to be molecularly engineered. Novel copolymers consisting of both a fluorocarbon and a hydrocarbon segment were synthesized earlier by Guan and DeSimone.[6]

Because of their wide specialty range and properties such as transparency and resistance to deterioration by environmental effects, acrylic polymers such as poly(methyl methacrylate) (PMMA) are used in a wide variety of applications, ranging from very soft adhesive materials to rigid non-film-forming products. In general, these acrylic polymers are prepared by conventional free-radical polymerization. Except for a few monomers (e.g., fluorinated oxetanes, oxazolines, and vinyl ethers that bear a fluorinated side group that currently homopolymerize cationically or hexafluoropropylene oxide and α-trifluoromethacrylic acid that polymerize under anionic conditions), most fluoropolymers are also synthesized from conventional radical methods of polymerization.[7–13] In practice, the free-radical polymerization method is used extensively because of the smooth processable conditions of vacuum and temperature, the ease of the process, the absence of residual catalyst in the final products, and the fact that the reactants do

not need to be highly pure as in the cases of cationic or anioninc polymerizations.

Because of the feasibility of radical polymerization, more than 50% of all plastics and more than 95% of fluoropolymers are prepared in this way.[14] Numerous different polymers with perfluorinated groups in the main chain or a side chain of acrylates, aromatic polyesters, and polyurethanes have been reported.[8,15–18] Also, the effects of the fluorinated side groups on the hydrophobic properties have been examined.[19–21] To achieve low-energy surfaces, many different fluorinated block copolymers with well-defined structures were synthesized; these include poly(ethylene oxide) and poly(perfluoroalkyl methacrylate), synthesized by atom transfer radical polymerization (ATRP), or polystyrene (pSt) initially prepared by living anionic polymerization.[22–29] ATRP polymerizations of different types of fluorinated monomers[22–27,30–34] (usually acrylates and methacrylates) in either conventional solvents or supercritical carbon dioxide[28] were realized to obtain various polymer architectures with controlled molecular weights (MWs), polydispersities, terminal functionalities, and compositions. 2-Perfluoroalkyl containing initiators have also been used in several ATRP reactions of copolymers.[10,35] A number of monosubstituted styrenes, for example, 4-fluoromethylstyrene and 4-trifluoromethylstyrene, or styrenic fluorinated monomers have been polymerized by free-radical polymerization or ATRP.[36–39] Also, the polymerization of fully phenyl fluorinated styrene, 2,3,4,5,6-pentafluorostyrene, and 2,3,5,6-tetrafluoro-4-methoxy styrene monomers has been successfully carried out via ATRP.[40–43] Recently, the originally synthesized highly fluorinated fluoroalkoxy styrene monomers 2,3,5,6-tetrafluoro-4-(2,2,3,3,3-pentafluoropropoxy) styrene and 2,3,5,6-tetrafluoro-4-(2,2,3,3,4,4,5,5,6,6,7,7,8,8,8-pentadecafluoroctaoxy) styrene were also used to produce polymers capable of forming low-surface-energy materials.[44] By the inclusion of fluorinated moieties in the initiators, semifluorinated pSt and PMMA copolymers have been obtained.[35,45] The initiators were different fluorinated bromoisobutyryl esters prepared by the esterification of various fluorinated telomers, such as perfluoroalkyl ethanol or 2-perfluoroalkyl ethyl–copoly(ethylene glycol), or a dihydroxy functional telomer based on trimethylol propane. We recently reported the synthesis of a new fluorinated initiator, 3,5 bis(perfluorobenzyloxy)benzyl 2-bromopropanoate bearing perfluorinated aromatic groups, and used this initiator to carry out the ATRP of styrene and methyl methacrylate (MMA) monomers.[46] It was found that pSt and PMMA with fluorinated end groups imparted high hydrophobic characteristics to the materials, even at low fluorine contents. The resulting chain-end fluorinated polymers exhibited higher hydrophobicity than the pure PMMA and pSt.

The polymerization of several different perfluorinated monomers, such as alkylic perfluorinated or styrene based monomers with fluorinated aromatic rings, has been performed successfully.[36–38] As an acrylic species, fluorinated aryl (meth)acrylates have also been investigated.[47–51]

In this study, the synthesized 3,5-bis(perfluorobenzyloxy)benzyl acrylate (FM) monomer was different from that in the literature; it bore more than one fluorinated phenyl ring, which contributed a more stiff structure to the polymer. Also, the FM monomer and its homopolymer or copolymers dissolved in most the common solvents easily, in contrast to most fluorinated polymers.

Consequently, a novel aromatic perfluorinated acrylate monomer and its MMA copolymers were synthesized, and the copolymerization behavior of this monomer with MMA was investigated. The kinetics of both monomers were studied to obtain information on the relationships among the structure, reactivity, and resulting properties. The synthesized monomers were characterized by ^{1}H-NMR, ^{19}F-NMR, and Fourier transform infrared (FTIR) spectroscopy. The obtained copolymers were characterized by ^{1}H-NMR, gel permeation chromatography (GPC), differential scanning calorimetry (DSC), and thermogravimetric analysis (TGA) methods. The surface features were examined by contact angle measurements.

EXPERIMENTAL

Materials

All solvents, acetone, tetrahydrofuran (THF), and dichloromethane, were purified and dried by standard techniques before use. Triethylamine (99%, Acros, Geel, Belgium), acryloylchloride (97%, Aldrich, Munich, Germany), pentafluorobenzyl bromide (98%, Alfa Aesar, Karlsruhe, Germany), 3,5-dihydroxybenzyl alcohol (99%, Aldrich, Munich, Germany), 18-crown-6 (99%, Merck, Brussels, Belgium), and 2,2′-azobisisobutyronitrile (AIBN; 99%, Aldrich, Munich, Germany) were used as received. MMA (98%, Fluka, Lyon, France) was purified by conventional methods and distilled *in vacuo* over CaH_2.

Characterization and analysis

FTIR spectra were measured with a model recorded PerkinElmer Spectrum One FTIR spectrophotometer Perkin Elmer, Boston, Massachusetts, USA (with an attenuated total reflectance sampling accessory). ^{1}H-NMR and ^{19}F-NMR spectra were obtained on a Bruker AC spectrometer, Bruker, Leipzig, Germany at 250 MHz and on a Varian Inova spectrometer, Varian, Darmstadt, Germany at 500 MHz, respectively, with $CDCl_3$ as the solvent. The chemical shifts are reported in parts per million from internal tetramethylsilane (TMS) (^{1}H-NMR) or from internal $CFCl_3$ (^{19}F-NMR). GPC analyses were carried out with a setup consisting of an Agilent, Akron, Ohio, USA, pump and refractive-index detector and three Agilent Zorbax PSM 1000S, 300S, and 60S columns (6.2 × 250 mm, 5 μ) measuring in the ranges 10^4–10^6, 3×10^3 to 3×10^5, and 5×10^2 to 10^4, respectively. THF was used as the eluent at a flow rate of 0.5 mL/min at 30°C. The MWs of the polymers were calculated with the aid of PMMA standards. The thermal properties of the polymers were measured by DSC (TA Instruments, New Castle, Delaware DSC Q10) in a flowing nitrogen atmosphere from 30°C at a scanning rate of 10°C/min. TGAs of the copolymers were performed with a TA Q50 and PerkinElmer Pyris1 thermogravimetric analyzers under nitrogen and air atmospheres, respectively. Samples were run from 30 to 800°C at a heating rate of 20°C/min. Scanning electron microscopy (SEM) imaging of the films were obtained with an FEI, Hillsboro, Oregon, Quanta 450 field emission gun (FEG) instrument. Contact angle measurements and surface free energy calculations were performed with a KSV Attension Theta Lite, Linthicum, Maryland, USA contact angle
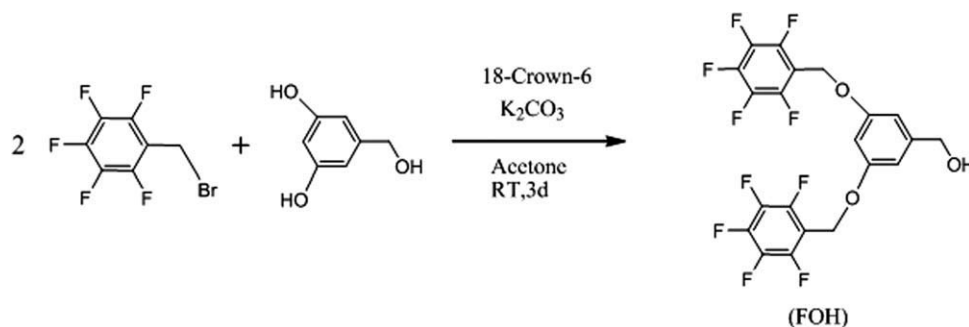
Scheme 1. Synthesis of FOH (RT = room temperature and 3d = 3 days).

instrument; deionized water and ethylene glycol drops (4–6 μL) were dispensed from a 1000-μL syringe. Contact angle measurements are reported as an average of three areas on different portions of the film surface. In this study, geometric mean approximations were used to obtain the dispersive and nondispersive contributions to the total surface energy. According to Owens and Wendt, the surface energy of a given solid can be determined with an equation applied to two liquids.[52]

Synthesis of 3,5-bis(perfluorobenzyl)oxybenzyl alcohol (FOH)
K_2CO_3 (3.52 g, 25.4 mmol) and 18-crown-6 (0.32 g, 1.21 mmol) were added, respectively, into mixtures of pentafluoro-benzyl bromide (6.62 g, 25.3 mmol) and 3,5-dihydroxybenzyl alcohol (1.71 g, 12.2 mmol) in acetone (100 mL) at room temperature and allowed to stir vigorously under nitrogen. After 3 days, the solvent was removed in vacuo, the residue was partitioned between water (20 mL) and CH_2Cl_2 (20 mL), the aqueous layer was extracted with CH_2Cl_2 (3 × 200 mL), and the CH_2Cl_2 extracts were combined, dried over $MgSO_4$, and concentrated in vacuo. The product, FOH, was obtained by crystallization from 50% hexane/CH_2Cl_2.

Yield = 72%, mp = 98°C. FTIR (v, cm^{-1}): 3292, 2896, 1659, 1597, 1524, 1456, 1378, 1286, 1130, 934, 828, 772, 687. ^{1}H–NMR (CDCl$_3$, δ, ppm): 2.16 (t, 1H), 4.66 (d, 2H), 5.10 (s, 4H), 6.47 (t, 1H), 6.64 (d, 2H). ^{19}F-NMR (CDCl$_3$, δ, ppm): −145.2 (m, 4F, ortho-F), −155.4 (m, 2F, para-F), −164.5 (m, 4F, meta-F).

Synthesis of FM
Under nitrogen, 2.02 mL (25 mmol) of acryloylchloride was added dropwise to a stirring mixture of FOH (8.34 g, 16.7 mmol) and triethylamine (3.51 mL, 25 mmol) in 180 mL of THF in an ice bath for 1 h. After the complete addition of the

acryoyl chloride, the reaction was stirred at room temperature for 15 h. The reaction mixture was subsequently washed with 0.1N hydrochloric acid, a saturated K_2CO_3 solution, saturated brine, diethyl ether, and deionized water. After the organic phase was dried with anhydrous Na_2SO_4, the solvent was removed; this resulted in a greasy yellow liquid. The product was further purified by column chromatography on silica (eluent: hexane/ethyl acetate = 4 : 1) to give the pure monomer.

Yield = 77%, mp = 50.8°C. FTIR (v, cm^{-1}): 2930, 1722, 1656, 1598, 1286, 1159, 937. ^{1}H-NMR (CDCl$_3$, δ, ppm): 6.7 (m, 2H), 6.5 (m, 1H), 6.4 (m, 1H), 6.2 (m, 1H), 5.8 (m, 1H), 5.1 (m, 2H), 5.0 (m, 4H). ^{13}C-NMR (CDCl$_3$, δ, ppm): 166.0, 159.4, 147.0, 140.1, 138.7, 131.8, 128.2, 109.8, 106.9, 102.0, 65.8, 57.4. ^{19}F-NMR (CDCl$_3$, δ, ppm): −145.2 (m, 4F), −155.2 (m, 2F), −164.5 (m, 4F).

Synthesis of the FM–MMA copolymers
The polymerizations were performed in a dry Schlenck tube that was charged with predetermined amounts of monomers (FM and MMA), 1 mL of toluene, and AIBN (2.5 mol % of the total monomer concentration). Oxygen was removed by three freeze–pump–thaw cycles by the application of a vacuum and backfilling with nitrogen. The tube with the polymerization mixture was immersed into a silicon oil bath preheated to 80°C. After the desired time, the tube was removed from the bath and cooled rapidly to ambient temperature, and the reaction mixture was diluted with THF. The polymers were precipitated into methanol and dried in vacuo. The yields were determined gravimetrically.

Film preparation
Thin polymer films were spin-coated (1000 rpm for 30 s) with a specialty coating systems (SCS) P6700, SCS Company,
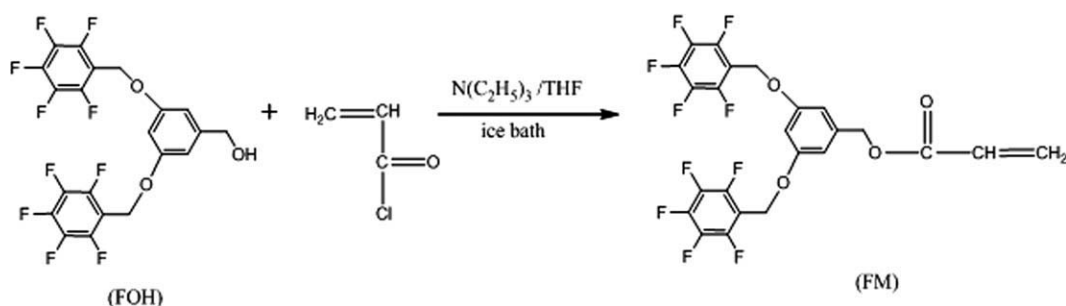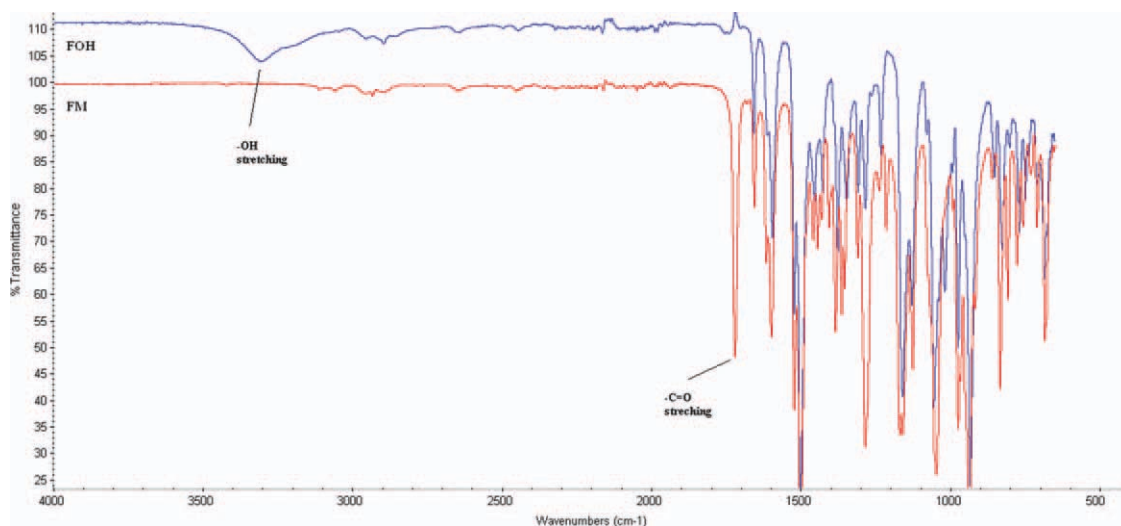

Scheme 2. Synthesis of FM.

Figure 1. FTIR spectra of FOH and FM. [Color figure can be viewed in the online issue, which is available at wileyonlinelibrary.com.]

Woodland Drive, Indianapolis, USA, spin coater onto a clean and dried glass substrate with solutions of the synthesized polymers with concentrations of 30 mg in 1 mL of dichloromethane. After spin coating, the polymer films were annealed for 2 h at 80°C in an oven. By this procedure, the glass substrate was completely covered with the polymers.

RESULTS AND DISCUSSION

In this study, perfluoroaromatic-group-containing acrylate copolymers in different compositions were synthesized via free-radical polymerization. For this purpose, FOH was used for the preparation of the fluorinated acrylate monomer. The reaction of 3,5-dihydroxybenzyl alcohol with α-bromopentafluorotoluene in the presence of K_2CO_3 and 18-crown-6 in acetone at room temperature for 3 days gave FOH in 72% yield (Scheme 1). Then, a perfluorinated aromatic group containing acrylate monomer (FM) was synthesized by the esterification of FOH with acryloylchloride (Scheme 2). The structure of the product FM was confirmed by spectroscopic investigations. The FTIR

spectrum showed no signal corresponding to —OH groups of the starting FOH at 3292 cm^{-1} and showed the characteristic C=O ester band at 1722 cm^{-1} (Figure 1).

In ^{1}H-NMR spectrum recorded in $CDCl_3$, the peak observed between at 5.8–6.4 ppm corresponded to monomeric H_2C=CH— protons. (Figure 2). The spectrum indicated the presence of two Ar—H protons at 6.6 ppm, two Ar—H protons at 6.7 ppm, and —OCH_2 Ar protons between at 5.0–5.3 ppm. The ^{19}F-NMR spectrum showed signals at −145.2, −155.2, and −164.4 ppm assigned to *ortho*-F, *para*-F, and *meta*-F atoms, respectively, in the aromatic ring (Figure 3).

Copolymers of the perfluorinated acrylate with MMA were synthesized by free-radical polymerization at 80°C under nitrogen, as shown in Scheme 3. The copolymerization parameters pointed to almost random copolymers. Table I lists the polymer characteristics of the prepared samples. The following notation is used for the different copolymers: poly[3,5-bis(perfluorobenzyloxy)benzyl acrylate] (pFM) and PMMA are the homopolymers of FM and MMA, respectively. p(FM-*co*-MMA)–50/50 represents a random copolymer of 50 mol % MMA and 50 mol % FM in the monomer feed. Thus, p(FM-*co*-MMA)–90/10 is a random copolymer of 90 mol % FM and 10 mol % MMA in the monomer feed. The copolymer compositions of the p(MMA-*co*-FM) copolymers were determined by ^{1}H-NMR. The
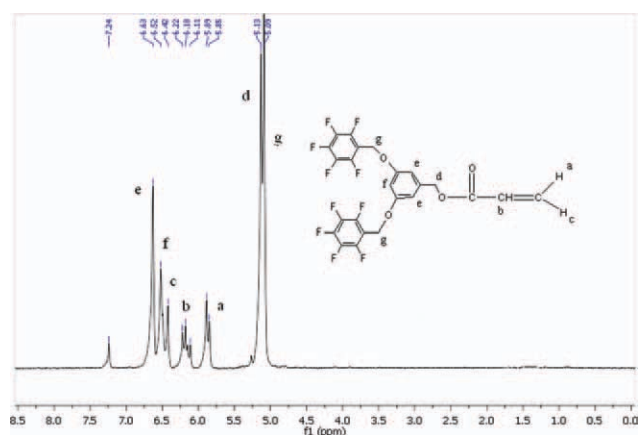

Figure 2. ^{1}H-NMR (in $CDCl_3$) spectrum of FM. [Color figure can be viewed in the online issue, which is available at wileyonlinelibrary.com.]
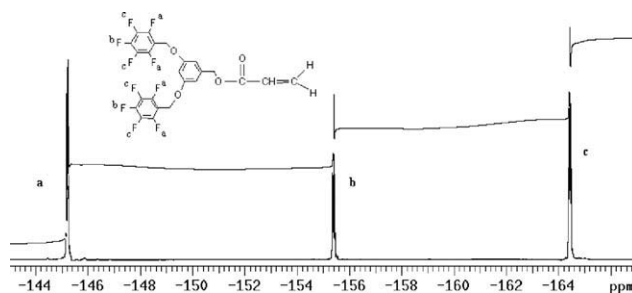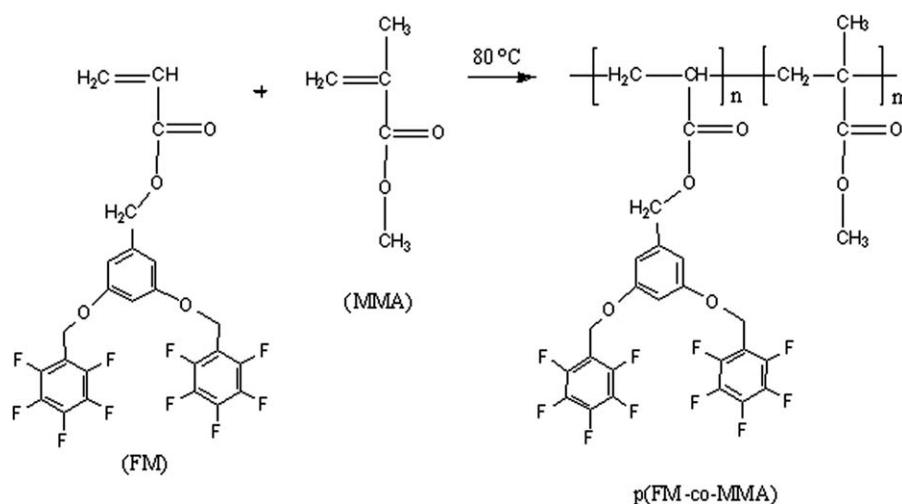

Figure 3. ^{19}F-NMR (in $CDCl_3$) spectrum of FM.

Scheme 3. Synthesis of the p(FM-*co*-MMA) copolymers.

experimental fraction of fluorinated monomers was slightly lower than the corresponding fraction in the monomer feed, as shown in Table I.

Figure 4 depicts the ^{1}H-NMR spectra of the pFM homopolymer and p(MMA-*co*-FM) copolymers. In the spectra, the peaks appearing around 6.2–6.8 ppm were assigned to the aromatic protons, and those around 4.90–5.00 ppm were assigned to —OCH$_2$ protons in the pFM polymer. The peaks between 0.80 and 2.5 ppm were assigned to —CH and —CH$_2$ protons in the polymer chains. The compositions of the copolymers (in Table I) were calculated on the basis of the ^{1}H-NMR results by comparison of the values of the integrals of the peaks appearing around 3.43–3.56 ppm, which is characteristic for —OCH$_3$ protons in the MMA monomer, and the peaks appeared in the range 6.2–6.8 ppm, which was for aromatic protons of the FM monomer.

The copolymerization of the newly synthesized fluorinated acrylic monomer (FM) with MMA was realized by free-radical polymerization with different monomer feeds to calculate the reactivity ratios of the monomers. For this purpose, during the copolymerizations, the total monomer composition and time

were maintained constant, and the temperature was maintained within ±0.1°C. All runs were carried out with the initiator at 2.5 mol % of the total monomer amount. Monomer reactivity ratios are important quantitative values for predicting the copolymer composition for any starting feed in batch, semibatch, and continuous reactors and for understanding the kinetic and mechanistic aspects of copolymerization.

A change in the reaction medium with conversion affects the monomer reactivity ratio values. Among several procedures available for determining the monomer reactivity ratio, the methods of Mayo–Lewis,[53] Finemann–Ross,[54] inverted Finemann–Ross, Kelen–Tüdos,[55] extended Kelen–Tüdos (EKT),[56–58] Tidwell–Mortimer,[59] and Mao–Huglin[60] are appropriate for the determination of the monomer reactivity ratios at low conversions. The EKT and Mao–Huglin methods consider the drift of comonomer and copolymer composition with conversion. Therefore, they are suitable for the manipulation of high-conversion data. For our system, the monomer reactivity ratios of MMA and FM for their free-radical copolymerization at 80°C were calculated by the well-known EKT method from the

Table I. Free-Radical Copolymerization of FM (M$_1$) and MMA (M$_2$) at 80°C.[a] f$_1$ and f$_2$ are the mol % copolymer composition of M$_1$ and M$_2$ in the copolymer, respectively, F$_1$ and F$_2$ are the mol % copolymer composition of M$_1$ and M$_2$ in the monomer feed respectively

	Monomer feed (mol %)		Copolymer composition (mol %)[b]				
	F$_1$	F$_2$	f$_1$	f$_2$	Conversion (%)	M$_n$[c]	M$_w$/M$_n$[c]
p(FM-*co*-MMA)–10/90	10	90	9	91	22	11,370	1.35
p(FM-*co*-MMA)–30/70	30	70	22	78	37	11,200	1.56
p(FM-*co*-MMA)–50/50	50	50	45	55	34	12,200	2.02
p(FM-*co*-MMA)–70/30	70	30	63	37	39	13,000	2.25
p(FM-*co*-MMA)–90/10	90	10	81	19	30	14,300	2.39
pFM	100	—	100	—	41	12,600	2.48
PMMA	—	100	—	100	11	14,100	1.19

M$_w$, weight-average molecular weight, [a]Initiator AIBN = 0.027M, [FM] + [MMA] = 1.08M, and time = 5 h, [b]Determined by ^{1}H-NMR data, [c]Determined by GPC measurement.
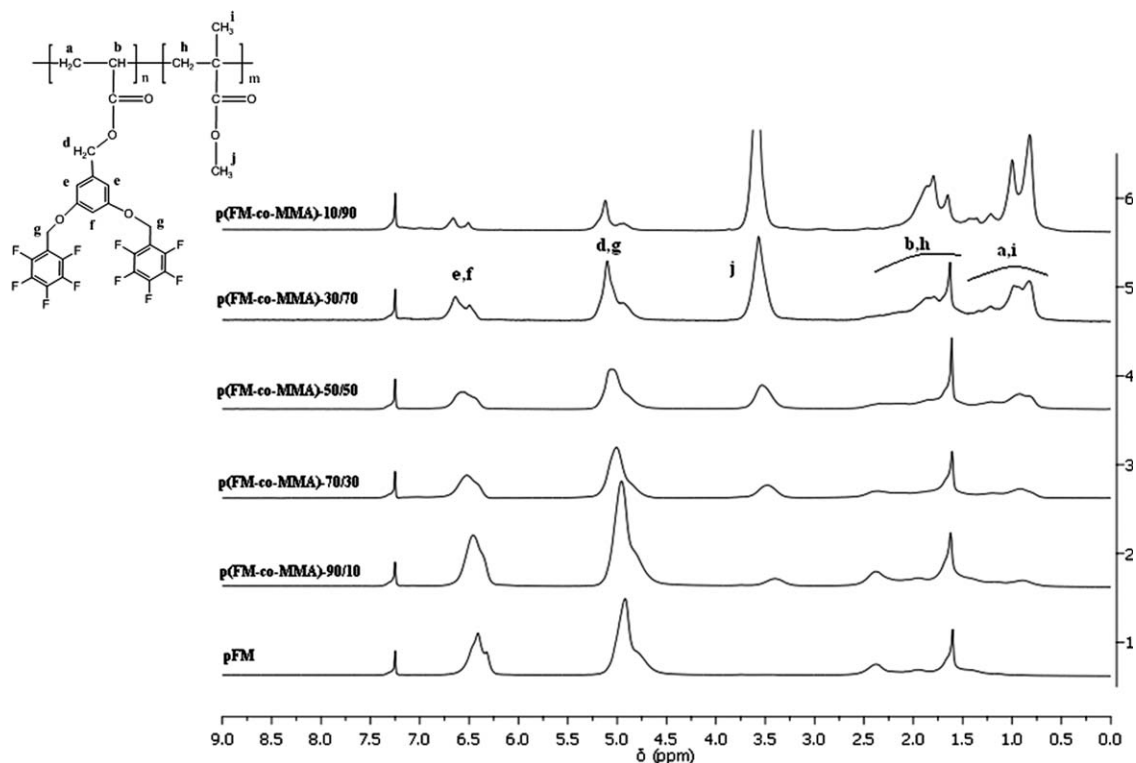
Figure 4. ^{1}H-NMR (in CDCl$_3$) spectrum of the p(FM-*co*-MMA) copolymers.

composition of the monomer feed and that of the instantaneously formed copolymer (Table II).

This method essentially uses the following equation

$$\eta = (r_1 + r_2/\alpha)\xi - r_2/\alpha \qquad (1)$$

where α is an arbitrary parameter and η and ξ are functions of both the feed and copolymer compositions and are defined as follows:

$$\eta = G/(H + \alpha) \text{ and } \xi = H/(H + \alpha) \qquad (2)$$

where H and G are defined with a conversion-dependent constant Z, which is expressed as follows:

$$Z = \log(1 - \xi_1)/\log(1 - \xi_2) \qquad (3)$$

where ξ_1 and ξ_2 are the partial molar conversions in monomers M_1 and M_2, respectively, and are given as follows:

$$\xi_1 = \xi_2(Y/X) \text{ and } \xi_2 = [\omega(\mu + X)]/(\mu + Y) \qquad (4)$$

where μ is the ratio of molecular weight of M_2 monomer (MMA) to M_1 monomer (FM), X is the ratio of mol % monomer feed of monomer 1 to monomer 2 and Y is the ratio of mol % copolymer composition of monomer 1 to monomer 2.

$$Y = f_1/f_2, \quad X = F_1/F_2, \quad \mu = \mu_2/\mu_1 \qquad (5)$$

where f_1 and f_2 are the mol % copolymer composition of FM (M_1) and MMA (M_2) respectively, F_1 and F_2 are the mol % co-

polymer composition in the monomer feed of M_1 and M_2 respectively, μ_1 and μ_2 represent the MWs of M_1 and M_2, respectively, x is the total fractional conversion. Thus, H and G are defined as follows:

$$H = Y/Z^2 \text{ and } G = (\gamma - 1)/Z \qquad (6)$$

where α is usually taken as

$$\alpha = (H_{max}, H_{min})^{1/2} \qquad (7)$$

where H_{max} and H_{min} are the maximum and minimum values of H coefficient, respectively. The monomer reactivity ratios (r_1 and r_2) were calculated with experimental data treated by the EKT method.[58,61] The linear plot according to eq. (1) gave $r_1 + r_2/\alpha$ as the slope and $-r_2/\alpha$ as the intercept (Figure 5).

The reactivity ratios, which were found to be $r_1 = 0.38$, $r_2 = 1.11$, and $r_1 r_2 < 1$ for the FM–MMA pair at 80°C, showed that this system underwent random copolymerization. The value of

Table II. EKT Parameters for the Monomer FM and MMA with ^{1}H-NMR

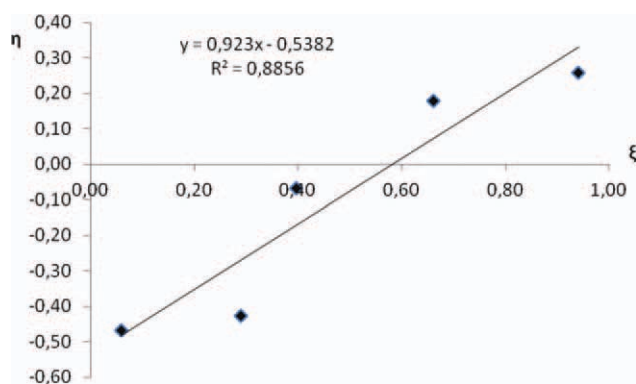| Run	Parameters of the EKT equation			
	H	G	ξ	η
p(FM-*co*-MMA)–10/90	0.13	−1.03	0.06	−0.47
p(FM-*co*-MMA)–30/70	0.84	−1.24	0.29	−0.43
p(FM-*co*-MMA)–50/50	1.36	−0.23	0.40	−0.07
p(FM-*co*-MMA)–70/30	4.03	1.08	0.66	0.18
p(FM-*co*-MMA)–90/10	33.01	9.08	0.94	0.26

Figure 5. EKT plots of ξ versus η for the free-radical copolymerization of FM (M_1) with MMA (M_2; $\alpha = 2.07$). [Color figure can be viewed in the online issue, which is available at wileyonlinelibrary.com.]

r_1 was less than 1; this meant that the FM-terminated propagating chain preferred to add MMA rather than another FM monomer that was involved in the reaction. According to the obtained results, we concluded that there occurred some compositional drift in which the produced copolymer contained more MMA than expected.

Reactive radicals formed during the polymerization tend to abstract hydrogen from the methylene group so there might have been some transfers from the methylene —OCH_2Ar of FM in the polymerization process. However, the abstraction of hydrogen would have been difficult because of the bulky pendant group, and it occurred in negligible amounts. If this was not the case, hyperbranched polymers would be formed, and our polymers would not have been easily dissolved in the solvents. The value of r_2 greater than unity implied that the copolymerization was initially dominated by this species, which was the more reactive monomer, as shown in Table I. The thermal behavior of the synthesized polymers was investigated with the DSC and TGA methods, and the observed results are summarized in Table III.

The homopolymer of fluorinated acrylate itself showed a glass-transition temperature (T_g) value of 49.6°C, and the obtained FM–MMA copolymers showed only one T_g value because it was a random copolymer. The T_g values of the copolymers ranged between 50 and 80°C. The highest T_g value (78°C) was obtained when the ratio of FM to MMA in the feed was 10 : 90 (Figure 6).

The T_g values of the copolymers was dependent on the copolymer composition. As shown in the DSC thermograms, the copolymers showed lower T_g values with increasing fluorinated monomer composition, although they had higher number-average molecular weight (M_n) values. This suggested that the introduction of perfluorinated groups in the polymer chain resulted in a plasticizing effect, and also, the bulky character of the aromatic rings provided a high free volume with a corresponding decrease of T_g. Instead of affecting the relative rigidity of the aromatic rings, flexible linkages such as —CH_2O— groups affected the glass-transition behavior by decreasing it. For all of these copolymers, no melting endotherms were observed under 300°C in the DSC traces. This indicated that the copolymers with all compositions were amorphous.

The thermal stability of the novel copolymers was investigated by TGA. Figures 7 and 8 show the weight loss of the FM–MMA copolymers as a function of the temperature in nitrogen and air atmospheres, respectively. In an attempt to compare the thermal stabilities of the different copolymers, residue values at 450°C, maximum weight loss temperatures, and weight changes for the first stage of decomposition are listed in Table III. All of the obtained copolymers underwent two-step degradation processes. For the p(FM-co-MMA)–10/90 and p(FM-co-MMA)–30/70 copolymers, decomposition in very early temperature range had onsets at 169 and 181°C, respectively; this was attributed to the volatilization of the entrapped moisture present in the copolymers and also to the degradation of the PMMA segment, which was the dominant monomer composition in the copolymer. The onset of the first major weight loss of the copolymers, which occurred around 316–340°C, corresponded to the onset decomposition of the ester linkages, mainly of the PMMA segment. The second major weight loss commenced at about 410°C; this coincided with the decomposition or condensation of aromatic rings of the pFM segment and the thermal cracking of benzyl ether linkages and the dehydrogenation process. As the fluorine content in the copolymer increased, the onset value of the first decomposition also increased with a decrease in the decomposition weight change. The synthesized copolymers had better thermal stability than the PMMA homopolymer. Char yields at 450°C increased as the molar percentage of FM monomer increased in the polymer chain, but the char yield of the pFM homopolymer was lower than those of some of the

Table III. DSC and TGA Results for the p(FM-co-MMA) Copolymers

Polymer	T_g (°C)	Maximum weight loss temperature of the first decomposition (°C)	Weight loss of the first decomposition (%)	Residue at 450°C (%)
PMMA	123	—	—	1
p(FM-co-MMA)–10/90	78	316	78	18
p(FM-co-MMA)–30/70	65	331	65	33
p(FM-co-MMA)–50/50	58	333	57	42
p(FM-co-MMA)–70/30	54	338	49	44
p(FM-co-MMA)–90/10	52	339	45	52
pFM	49	343	41	53
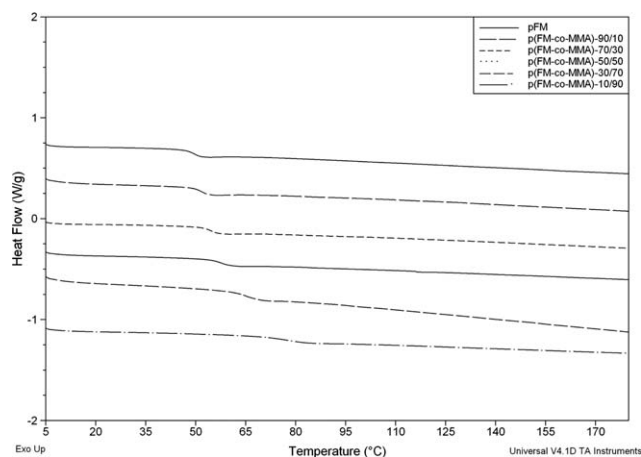
Figure 6. DSC thermograms of the p(FM-*co*-MMA) copolymers.

Figure 7. TGA thermograms of the p(FM-*co*-MMA) copolymers under a nitrogen atmosphere.

copolymers because of its lower MW. The introduction of fluorinated monomer into the copolymer was expected to improve their thermal stability.

The thermal stabilities of pFM, PMMA, and some of the copolymer samples [p(FM-*co*-MMA)–50/50 and p(FM-*co*-MMA)–10/90] were also evaluated under an air atmosphere as a comparison. It is shown in Figure 8 that they showed similar behavior in a nitrogen atmosphere, except for the char yield. Under an air atmosphere at 450°C, the char yields of PMMA, p(FM-*co*-MMA)–10/90), p(FM-*co*-MMA)–50/50, and pFM were 2, 14, 44, and 55%, respectively; these values were slightly higher than those in a nitrogen atmosphere.

Under air after 600°C, the ash contents of the copolymers decreased to below 5%. The results suggest that an oxidative environment enhanced the ignition characteristics and led to a
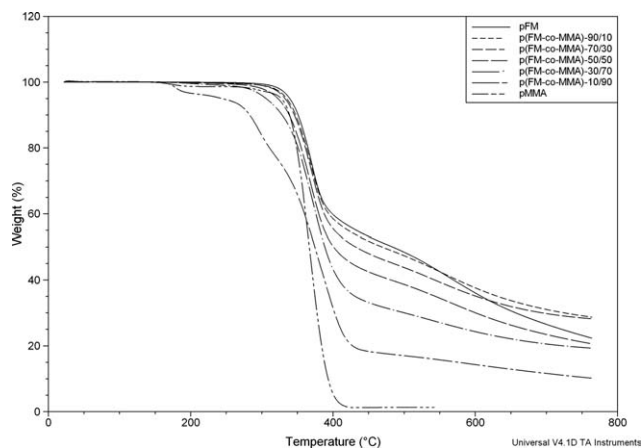
more rapid weight loss. Figure 9 shows the SEM images of the surfaces of the copolymer films that contained 10, 50, and 70% fluorinated monomer.

We observed from the SEM micrographs that the fluorine segments were dispersed throughout the polymer film surface. Because of the relatively low surface energy, the fluorinated monomer had a tendency to move toward the film surface as the percentage of FM monomer increased. A thicker fluorine-rich surface layer might have formed on the films with higher FM contents as the fluorinated polymer chains segregated toward the polymer–air interface. The phase contrast was not so sharp, and wormlike cocontinuous domains were seen. These domain structures were qualitatively similar to the microphase separation expected for segmented copolymers. To investigate the effect of the perfluorinated aromatic group on the surface
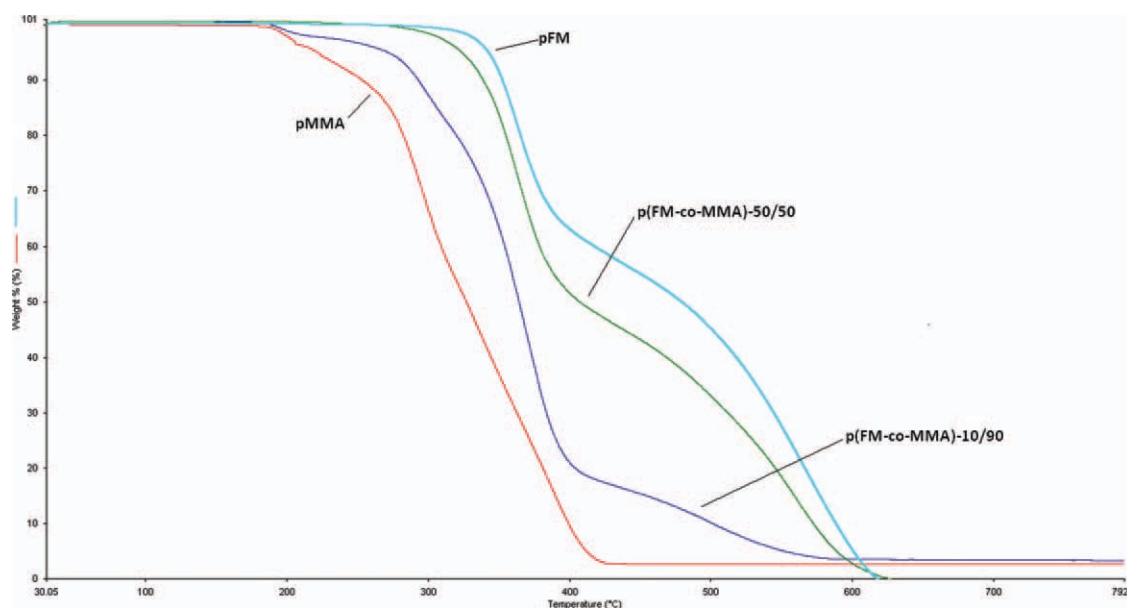

Figure 8. TGA thermograms of pFM, PMMA homopolymers, and the p(FM-*co*-MMA)–50/50 and p(FM-*co*-MMA)–10/90 copolymers under an air atmosphere. [Color figure can be viewed in the online issue, which is available at wileyonlinelibrary.com.]
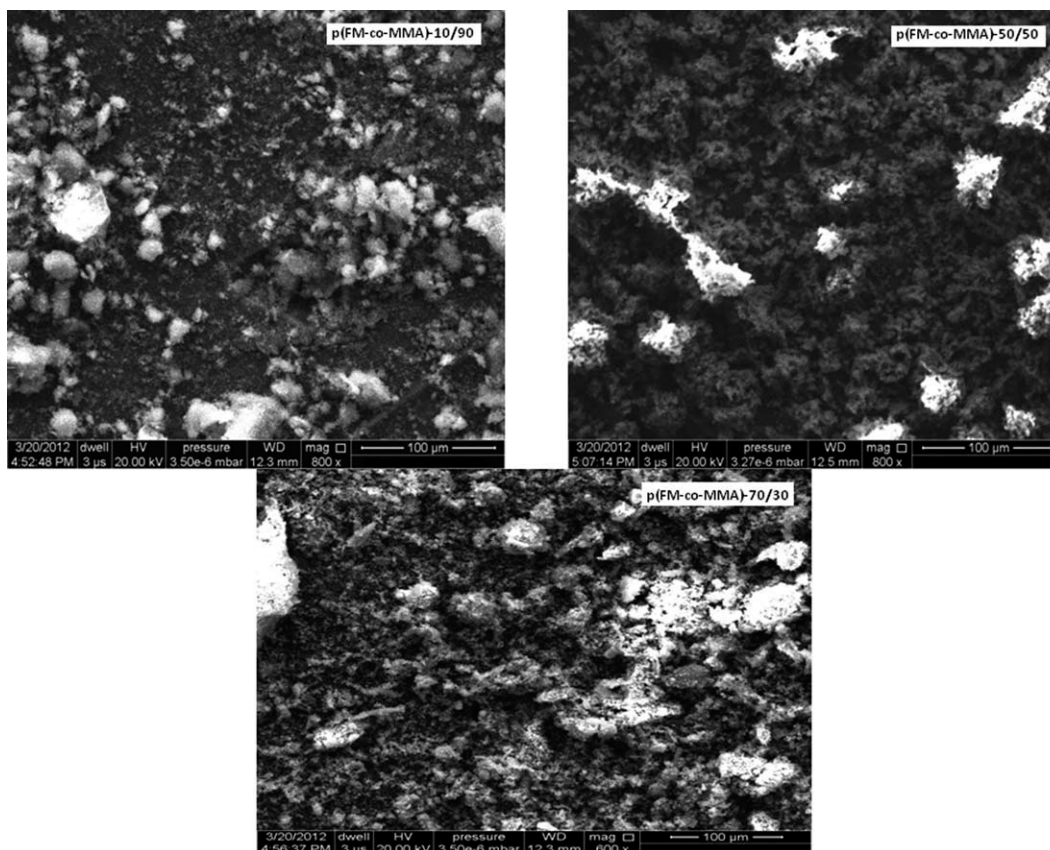
Figure 9. SEM images of the p(FM-*co*-MMA)–50/50, p(FM-*co*-MMA)–10/90, and p(FM-*co*-MMA)–70/30 copolymer films.

properties of the copolymers, contact angle measurements were performed with deionized water and ethylene glycol as wetting agents. The surface free energy values of the films were calculated from the average contact angles. An Owens–Wendt geometric mean with the two-liquid method[52,62] was applied. As shown in Figure 10, with the introduction of the fluorinated monomer to the MMA polymer, the surface of the polymer became hydrophobic. As expected, the surface tension of the films of the p(FM-*co*-MMA) copolymers decreased with increasing molar fraction of the fluorinated acrylic monomer in the chain.

The advancing and receding contact angles (θ_{adv} and θ_{rec}, respectively) of water were measured for all polymer films to determine the relative hydrophobicity of the surface. Table IV gives average contact angles for the fluorinated films, along with the values for PMMA and pFM polymer films for comparison.

Fluorinated compounds, including commercially available polymers, have been used as macroinitiators for nonfluorinated monomers to incorporate fluorinated species into the polymer chain. Recently, our group developed a novel type of fluorinated initiator that was used for the polymerization of styrene and MMA to afford polymers possessing fluorinated chain ends.[63] The monomer (FM) synthesized in this study was a derivative of that initiator, and its polymers had better nonwetting properties with higher contact angle values. The synthesized perfluori-

nated aryl acrylate (FM) monomer was effective for the surface hydrophobicity as was the the perfluorinated alkylic or perfluorinated styrenic monomers in the literature.[29,64,65] It was different from the synthesized fully phenyl fluorinated styrene monomers in the literature because it was an acrylate monomer with two perfluorinated phenyl rings contributing a more stiff structure to the polymers, so it could be used for multipurpose
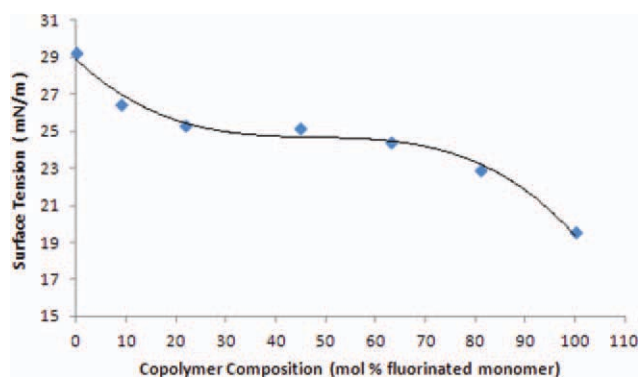

Figure 10. Surface energy values of the p(FM-*co*-MMA) copolymers as a function of the molar fraction of the fluorinated monomer unit in the polymer chain. [Color figure can be viewed in the online issue, which is available at wileyonlinelibrary.com.]

Table IV. Surface Properties of the Spin-Cast Polymer Films

| | Surface free energy (mN/m) | | | θ (°) with | | | |
| | | | | Deionized water | | Ethylene glycol | |
	γ_s^p	γ_s^d	γ_s	θ_{adv}	θ_{rec}	θ_{adv}	θ_{rec}
PMMA	28.20	1.07	29.27	85	59	63	45
p(FM-co-MMA)–10/90	12.39	14.07	26.45	95	67	72	48
p(FM-co-MMA)–30/70	23.95	1.37	25.32	99	74	75	50
p(FM-co-MMA)–50/50	21.71	3.46	25.17	100	78	78	54
p(FM-co-MMA)–70/30	14.14	10.30	24.44	101	77	76	56
p(FM-co-MMA)–90/10	18.49	4.38	22.86	104	79	82	55
pFM	16.77	2.79	19.53	106	82	83	68

γ_s^d, dispersion component; γ_s^p, polar (nondispersion) component; γ_s, surface energy.

coating applications, such as outdoor water-resistant coatings. Also, as an advantage, the FM monomer and its homopolymer or copolymers dissolved in most common solvents easily, in contrast to most of the fluorinated polymers. Among the unique properties of fluorinated polymers, they have a low water absorption. PMMA had a tendency to absorb water; however, when the FM monomer was incorporated into MMA, the absorption was greatly decreased.

A typical water absorption tendency of the copolymer of p(FM-co-MMA)–10/90 is shown in Figure 11. Even for a 9 mol % FM content in the copolymer, the water absorption was found to decrease one-third compared with that of pure PMMA. The decreasing water absorption could have resulted from the hydrophobic surface and bulkiness of the copolymer containing fluorinated aromatic rings. As it is known, the difference between the advancing and receding contact angles is called the *hysterese*. The hysteresis gives information about the surface roughness and the inhomogeneity in the surface. The advancing contact angle changed significantly from 85 to 104° as the fluorine content increased, but the hysteresis did not change much; this suggested that the surface of the film did not become rough and/or chemically heterogeneous.
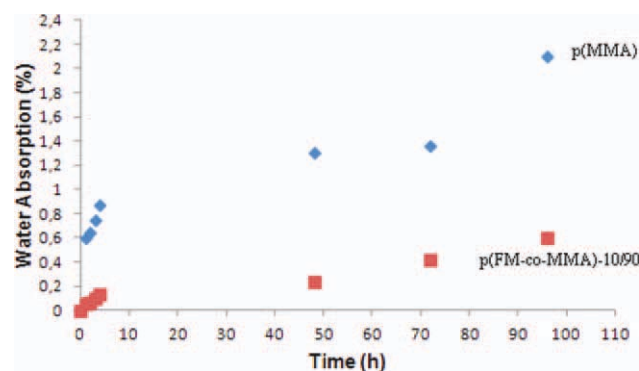
CONCLUSIONS

We demonstrated the successful synthesis and polymerization of a new aromatic perfluorinated acrylic monomer and its copolymerization with MMA. The reactivity of MMA was found to be slightly larger than that of FM according to the reactivity ratios determined by the EKT method. The greatest challenge of synthesizing novel fluorinated monomers is often the analysis of the final products because of their low solubility, but in this study, the homopolymers of the synthesized monomer and copolymers were soluble in organic solvents such as THF, dichloromethane, acetone, and dimethyl sulfoxide. In the DSC measurements, only one T_g was observed for each copolymer. These results indicate that the monomers FM and MMA had good copolymerization tendencies and that nearly ideal random copolymers were prepared via their copolymerization. The addition of fluorinated side groups to the copolymer resulted in a hydrophobic surface. Furthermore, the critical surface tensions of the fluorinated copolymer films were lower than that of PMMA. These properties made the copolymers good candidates for hydrophobic optical, electrical, and coating materials. The synthesis of homopolymers and block copolymers of this monomer (FM) via controlled radical polymerizations has been studied and will be presented in the future.

Figure 11. Water absorption of pure PMMA and p(FM-co-MMA)–10/90. [Color figure can be viewed in the online issue, which is available at wileyonlinelibrary.com.]

REFERENCES

1. Otsu, T.; Matsumoto, A.; Kubota, T.; Mori, S. *Polym. Bull.* **1990,** *23*, 43.

2. Banks, R. E.; Smart, B. E.; Tatlow, J. C. Organofluorine Chemistry: Principles and Commercial Applications; Plenum: New York, 1994.

3. Pierandrea, L. N. *Adv. Colloid. Interface. Sci.* **1995,** *56*, 245.

4. Castelvetro, V.; Aglietto, M.; Ciardelli, F.; Spagnoli, F. *J. Fluorine. Chem.* **2004,** *125*, 315.

5. Pilati, F.; Toselli, M.; Re, A.; Bottino, F. A.; Pollicino, A.; Recca, A. *Macromolecules* **1990,** *23*, 348.

6. Guan, Z.; DeSimone, J. M. *Macromolecules* **1994,** *27*, 5527.

7. Ebnesajjad, S.; Khaladkar, P. R. Fluoropolymers Applications in Chemical Processing Industries: The Definitive User's Guide and Databook; William Andrew: Norwich, NY, 2004.

8. Scheirs, J. Modern Fluoropolymers: High Performance Polymers for Diverse Applications; Wiley: New York, 1997.

9. Hougham, G. Fluoropolymers: Synthesis; Kluwer Academic/Plenum: New York, 1999.

10. Améduri, B.; Boutevin, B. Well-Architectured Fluoropolymers: Synthesis, Properties and Applications; Elsevier: Amsterdam, 2004.

11. Ameduri, B.; Boutevin, B. *J. Fluorine. Chem.* **2005,** *126*, 221.

12. Taguet, A.; Ameduri, B.; Boutevin, B. In Advances in Polymer Science; Ameduri, B., Ed.; Crosslinking in Materials Science 184; Springer: New York, **2005;** p 127.

13. Xu, Q.; Frisch, H. L. *J. Polym. Sci. Part A: Polym. Chem.* **1994,** *32*, 2803.

14. Bruno, A. *Macromolecules* **2010,** *43*, 10163.

15. Guyot, B.; Ameduri, B.; Boutevin, B. *J. Fluorine. Chem.* **1995,** *74*, 233.

16. Guyot, B.; Ameduri, B.; Boutevin, B.; Sideris, A. *Macromol. Chem. Phys.* **1995,** *196*, 1875.

17. Guyot, B.; Ameduri, B.; Boutevin, B.; Melas, M.; Viguier, M.; Collet, A. *Macromol. Chem. Phys.* **1998,** *199*, 1879.

18. Guyot, B.; Boutevin, B.; Ameduri, B. *Macromol. Chem. Phys.* **1996,** *197*, 937.

19. Ameduri, B.; Bongiovanni, R.; Lombardi, V.; Pollicino, A.; Priola, A.; Recca, A. *J. Polym. Sci. Part A: Polym. Chem.* **2001,** *39*, 4227.

20. Bongiovanni, R.; Pollicino, N.; Gozzelino, G.; Malucelli, G.; Priola, A.; Ameduri, B. *Polym. Adv. Technol.* **1996,** *7*, 403.

21. Ameduri, B.; Bongiovanni, R.; Malucelli, G.; Pollicino, A.; Priola, A. *J. Polym. Sci. Part A: Polym. Chem.,* **1999,** *37*, 77.

22. Iyengar, D. R.; Perutz, S. M.; Dai, C.-A.; Ober, C. K.; Kramer, E. J. *Macromolecules* **1996,** *29*, 1229.

23. Wang, J.; Mao, G.; Ober, C. K.; Kramer, E. J. *Macromolecules* **1997,** *30*, 1906.

24. Böker, A.; Reihs, K.; Wang, J.; Stadler, R.; Ober, C. K. *Macromolecules* **2000,** *33*, 1310.

25. Sugiyama, K.; Nemoto, T.; Koide, G.; Hirao, A. *Macromol. Symp.* **2002,** *181*, 135.

26. Hirao, A.; Koide, G.; Sugiyama, K. *Macromolecules* **2002,** *35*, 7642.

27. Andruzzi, L.; Chiellini, E.; Galli, G.; Li, X. F.; Kang, S. H.; Ober, C. K. *J. Mater. Chem.* **2002,** *12*, 1684.

28. Böker, A.; Herweg, T.; Reihs, K. *Macromolecules* **2002,** *35*, 4929.

29. Hirao, A.; Sugiyama, K.; Yokoyama, H. *Prog. Polym. Sci.* **2007,** *32*, 1393.

30. Wang, J.; Ober, C. K. *Macromolecules* **1997,** *30*, 7560.

31. Li, K.; Wu, P.; Han, Z. *Polymer* **2002,** *43*, 4079.

32. Hussain, H.; Budde, H.; Höring, S.; Busse, K.; Kressler, J. *Macromol. Chem. Phys.* **2002,** *203*, 2103.

33. Hussain, H.; Busse, K.; Kressler, J. *Macromol. Chem. Phys.* **2003,** *204*, 936.

34. Lim, K. T.; Lee, M. Y.; Moon, M. J.; Lee, G. D.; Hong, S.-S.; Dickson, J. L.; Johnston, K. P. *Polymer* **2002,** *43*, 7043.

35. Perrier, S.; Jackson, S. G.; Haddleton, D. M.; Améduri, B.; Boutevin, B. *Macromolecules* **2003,** *36*, 9042.

36. Lou, L.; Koike, Y.; Okamoto, Y. *J. Polym. Sci. Part A: Polym. Chem.* **2010,** *48*, 4938.

37. Qiu, J.; Matyjaszewski, K. *Macromolecules* **1997,** *30*, 5643.

38. Valade, D.; Boschet, F.; Ameduri, B. *J. Polym. Sci. Part A: Polym. Chem.* **2011,** *49*, 4668.

39. Irita, T.; Chen, D.; Li, X.; Wang, J.; Russell, T. P. *Macromol. Chem. Phys.* **2011,** *212*, 2399.

40. Jankova, K.; Hvilsted, S. *Macromolecules* **2003,** *36*, 1753.

41. Johnson, J. A.; Gudipati, C. S.; Wooley, K. L. *Polym. Prepr. (Am. Chem. Soc. Div. Polym. Chem.)* **2003,** *44*, 238.

42. Hvilsted, S.; Borkar, S.; Abildgard, L.; Georgieva, V.; Siesler, H. W.; Jankova, K. *Polym. Prepr. (Am. Chem. Soc. Div. Polym. Chem.)* **2002,** *43*, 26.

43. Hvilsted, S. R.; Borkar, S.; Siesler Heinz, W.; Jankova, K. In Advances in Controlled/Living Radical Polymerization Vol. *854*; Matyjaszewski, K., Ed.; American Chemical Society: Washington, DC, **2003;** p 236.

44. Borkar, S.; Jankova, K.; Siesler, H. W.; Hvilsted, S. *Macromolecules* **2004,** *37*, 788.

45. Perrier, S.; Jackson, S. G.; Haddleton, D. M.; Ameduri, B.; Boutevin, B. *Tetrahedron* **2002,** *58*, 4053.

46. Canak, T. C.; Kizilcan, N.; Serhatli, I. E. *J. Appl. Polym. Sci.* **2011,** *119*, 183.

47. Hansen, N. M. L.; Jankova, K.; Hvilsted, S. *Eur. Polym. J.* **2007,** *43*, 255.

48. Theato, P. *J. Polym. Sci. Part A: Polym. Chem.* **2008,** *46*, 6677.

49. Atanasov, V.; Kerres, J. *Macromolecules* **2011,** *44*, 6416.

50. Eberhardt, M.; Mruk, R.; Zentel, R.; Théato, P. *Eur. Polym. J.* **2005,** *41*, 1569.

51. Teng, H.; Yang, L.; Mikes, F.; Koike, Y.; Okamoto, Y. *Polym. Adv. Technol.* **2007,** *18*, 453.

52. Owens, D. K.; Wendt, R. C. *J. Appl. Polym. Sci.* **1969,** *13*, 1741.

53. Mayo, F. R.; Lewis, F. M. *J. Am. Chem. Soc.* **1944,** *66*, 1594.

54. Fineman, M.; Ross, S. D. *J. Polym. Sci.* **1950,** *5*, 259.

55. Kelen, T.; TÜds, F. *J. Macromol. Sci. Chem.* **1975,** *9*, 1.

56. Tüdos, F.; Kelen, T.; Földes-berezsnich, T.; Turcsányi, B. *J. Macromol. Sci. Chem.* **1976,** *10*, 1513.

57. Kelen, T.; Tüdöus, F.; Turcsányi, B.; Kennedy, J. P. *J. Polym. Sci. Polym. Chem. Ed.* **1977,** *15*, 3047.

58. Tüdös, F.; Kelenm, T. *J. Macromol. Sci. Chem.* **1981,** *16*, 1283.

59. Tidwell, P. W.; Mortimer, G. A. *J. Polym. Sci. Part A: Gen. Pap.* **1965,** *3*, 369.

60. Mao, R.; Huglin, M. B. *Polymer* **1993,** *34*, 1709.

61. Nair, C. P. R.; Mathew, D.; Ninan, K. N. *Eur. Polym. J.* **1999,** *35*, 1829.

62. Kinloch, A. J. Adhesion and Adhesives: Science and Technology; Chapman & Hall: London, 1987.

63. Çanak, T. Ç.; Selçukoğlu, M.; Hamuryudan, E.; Serhatlı, İ. E. *J. Appl. Polym. Sci.* **2012,** *124*, 1683.

64. Martinelli, E.; Paoli, F.; Gallot, B.; Galli, G. *J. Polym. Sci. Part A: Polym. Chem.* **2010,** *48*, 4128.

65. Martinelli, E.; Fantoni, C.; Gallot, B.; Glisenti, A.; Galli, G. *Macromol. Symp.* **2010,** *296*, 294.